Spatiotemporal Variations of NO_2 over Fukuoka Japan, Observed by Multiple MAX-DOAS and 3-D Coherent Doppler Lidar

Hironobu Ueki[1], Hisahiro Takashima[2], and Martina Michaela Friedrich[3]
[1]*Graduate School of Science, Fukuoka University, Fukuoka, Japan*
[2]*Faculty of Science, Fukuoka University, Fukuoka, Japan*
[3]*Belgian Institute for Space Aeronomy, Brussels, Belgium*

Abstract

To clarify three-dimensional (3-D) spatiotemporal variations and horizontal–vertical transport processes in nitrogen dioxide (NO_2) over urban areas, combined NO_2 profile observations by multiple Multi AXis Differential Optical Absorption Spectroscopy (MAX-DOAS) and direct wind observations by 3-D coherent Doppler lidar were made over an urban area in Japan. MAX-DOAS measurements were conducted at Yakuin and Fukuoka University in Fukuoka urban area with high temporal resolution of four minutes.

Enhanced NO_2 concentrations were often observed over the city center. We conducted a case study on 29 November 2018 under clear sky conditions and NO_2 profiles were well retrieved. Using MAX-DOAS at two locations, high NO_2 concentrations were observed near the surface of the city center in the morning. Higher NO_2 concentrations appearing gradually at higher altitudes over the city center and disappearing in the afternoon are explained using direct evidence of a 3-D wind field: an airmass with a high NO_2 concentration was transported upward over the city center. Then, the airmass was advected landward by a sea breeze. Multiple MAX-DOAS combined with 3-D Doppler lidar constitutes a powerful tool for elucidating horizontal–vertical transport processes. It can contribute to the improvement of data retrieval by satellites for urban areas.

(**Citation**: Ueki, H., H. Takashima, and M. M. Friedrich, 2021: Spatiotemporal variations of NO_2 over Fukuoka Japan, observed by multiple MAX-DOAS and 3-D coherent Doppler lidar. *SOLA*, **17**, 69−73, doi:10.2151/sola.2021-011.)

1. Introduction

Nitrogen oxides (NO_x = NO + NO_2) strongly affect air quality. They are expected to play a key role in climate change in the troposphere (e.g., Solomon et al. 1999). Elucidating tropospheric NO_2 variation in urban areas to enhance our knowledge of atmospheric chemistry is important because spatial variations in NO_2 concentrations are large there as a result of the spatial complexity of emission sources and short photochemical lifetimes of hours to days (e.g., Lamsal et al. 2010; Miyazaki et al. 2012; Takashima et al. 2015; Yamaguchi et al. 2016).

Tropospheric NO_2 measurements have long been conducted by satellite (e.g., Boersma et al. 2004; Richter et al. 2005; Boersma et al. 2011; Hilboll et al. 2013). In recent years, satellite observations have been developed to have finer spatial resolution, e.g., 5.5 × 3.5 km^2, for the Sentinel-5 Precursor/TROPospheric Ozone Monitoring Instrument (TROPOMI) satellite (Veefkind et al. 2012); it can be a powerful tool for elucidating the atmospheric environment in urban area. To validate the satellite tropospheric NO_2, ground-based Multi AXis Differential Optical Absorption Spectroscopy (MAX-DOAS) has been used (e.g., Brinksma et al. 2008; Irie et al. 2008b; Valks et al. 2011; Ma et al. 2013; Kanaya et al. 2014; Pinardi et al. 2020). This passive remote sensing technique is designed for atmospheric aerosol and gas profile measurements using scattered visible and ultraviolet solar radiation at several elevation angles (e.g., Höenninger et al. 2004; Wagner et al. 2004; Wittrock et al. 2004; Sinreich et al. 2005; Frieß et al. 2006; Irie et al. 2011). Because MAX-DOAS has high sensitivity to NO_2 near the ground, it can measure the NO_2 profile continuously during the daytime.

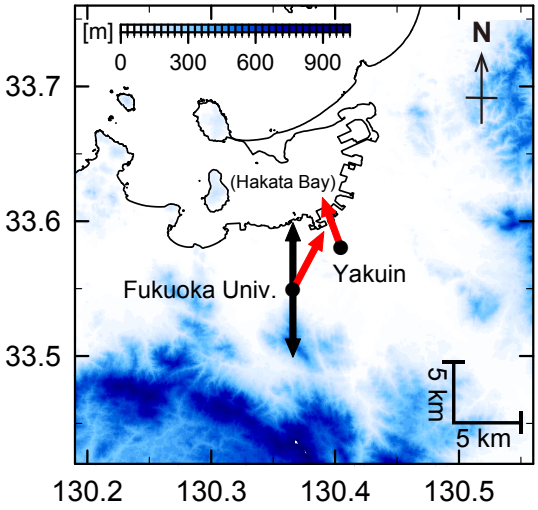

Fig. 1. Locations of observatories (longitude–latitude section). Color shows altitude; the solid line represents the coastline. Black arrows indicate the azimuth directions for RHI scanning of 3-D CDL. Red arrows represent lines of sight of MAX-DOAS.

To clarify three-dimensional (3-D) spatiotemporal variations and horizontal–vertical transport processes affecting NO_2 over urban areas, MAX-DOAS measurements were taken from October 2018 with high temporal resolution of four minutes at two observatories in Fukuoka city, an urban area in Japan: Yakuin (33.58°N, 130.40°E) and Fukuoka University (33.55°N, 130.36°E). The distance between Yakuin and Fukuoka University is approximately 4.5 km, which is roughly equivalent to the spatial resolution of TROPOMI (Fig. 1). Although many past studies have been conducted with particular emphasis on transport processes of trace gases and pollutants, most studies have been based on surface observations. Observation methods for vertical profiles of trace gas, such as MAX-DOAS, have been developed in recent decades.

Fukuoka city, located on the Fukuoka plain south of Hakata Bay, has a population of approximately 1.6 million people concentrated in the city center. In contrast to other large cities in Japan, no large city is near Fukuoka city, making it an ideal location for elucidating the spatiotemporal variation of NO_2, particularly for the transport and dilution processes of pollutants emitted from the city itself.

In earlier studies, a two-axis type MAX-DOAS instrument and car-mounted type MAX-DOAS instrument were used in Fukuoka city to clarify the inhomogeneity of NO_2 (Takashima et al. 2015; Yamaguchi et al. 2016). Results of those studies show

Corresponding author: Hisahiro Takashima, Faculty of Science, Fukuoka University, 8-19-1 Nanakuma, Jonan-ku, Fukuoka 814-0180, Japan. E-mail: hisahiro@fukuoka-u.ac.jp.

that spatiotemporal variations of NO_2 are consistent with a sea-breeze circulation system by surface wind observations. Nevertheless, they merely deduced transport processes through surface wind observations, without direct observational evidence. For the present study, we conducted NO_2 profile observations at two locations together with direct 3-D wind observations, providing direct observational evidence for horizontal and vertical transport processes of an airmass with high NO_2 concentration emitted from Fukuoka city.

We have been conducting observations using a 3-D coherent Doppler lidar (3-D CDL) installed at Fukuoka University (33.55°N, 130.37°E; 55 m above sea level) since 30 November 2016 (Takashima et al. 2019). From those observations, we have analyzed data for continuous 3-D wind and signal-to-noise ratio (SNR) (approximately proportional to aerosol concentration). Data from 3-D wind observations can clarify horizontal–vertical transport processes of airmasses enriched with NO_2 from near surface emission sources on small spatial scales.

The NO_2 profiles retrieved from MAX-DOAS observations often show enhanced NO_2 concentrations above the city center throughout the year. The simultaneous observations made using MAX-DOAS at the two locations together with 3-D CDL are limited. In addition, limiting the coincident periods to those with clear sky conditions and availability of lidar measurements with at least a certain SNR leaves very few days. Consequently, for this investigation, to clarify spatiotemporal variations in NO_2, we conducted a case study of 29 November 2018 as the best example, when the NO_2 profiles at two locations were well retrieved at different times throughout the day. We also compared the tropospheric NO_2 vertical column densities (NO_2VCD) observed using TROPOMI with retrieved results from measurements taken with multiple MAX-DOAS instruments.

2. Observations

2.1 NO_2 profile observations made using multiple MAX-DOAS instruments

For this study, NO_2 profile observations were made with MAX-DOAS instruments at Yakuin (33.58°N, 130.40°E) and at Fukuoka University (33.55°N, 130.36°E), located respectively about 1 km southwest of the city center (Tenjin) and about 5 km southwest of the city center (Fig. 1). Yakuin is located inside the urban area. The line of sight of the telescope is seaward (Hakata Bay). Fukuoka University is located far from the city center, but the telescope line of sight is toward the city center. It is noteworthy that the MAX-DOAS instrument at Fukuoka University obtains NO_2 profiles over the city center.

The MAX-DOAS instrument consists of two main parts: an outdoor telescope unit (Fig. S1) and an indoor spectrometer unit. The instrument is designed to be compact and to be operated with low power (up to 60 W). The telescope rotates to observe scattered sunlight at elevation angles of 2°, 3°, 4°, 5°, 10°, 20°, 30°, and 90° (elevation angles are changed every 30 s). The NO_2 profile is obtained with temporal resolution of 4 min. The telescope field of view is < 0.6°. A seven-core (100 μm radii) fiber optic bundle cable connects the outdoor telescope unit to the indoor spectrometer unit. The indoor spectrometer unit consists of the spectrometer (USB 4000; Ocean Optics Inc.) and a computer for spectral data recording and telescope elevation angle control. The spectrometer is housed in a heat-insulating plastic box to keep the spectrometer temperature at 288 ± 0.1 K using a temperature controller (E5CC; Omron Corp.) with a Peltier cooler. The spectral resolution of full-width at half-maximum (FWHM) is approximately 0.6 nm.

The recorded spectra for 460−490 nm are analyzed using the DOAS technique (Platt 1994) to retrieve the differential slant column densities (DSCD) of the oxygen collision complex (O_2−O_2 or O_4) and NO_2, as reported by Irie et al. (2011). Here, DSCD is defined as the difference between the column concentration integrated along the sunlight path measured at low elevation angles and at a midday reference elevation angle (90°). Absorption by NO_2, O_4, O_3, H_2O, and the Ring effect were considered. We used the NO_2 absorption cross-section data at 294 K reported by Vandaele et al. (1996), O4 at 296 K by Thalman et al. (2013), O_3 at 243 K by Bogumil et al. (2003), and H_2O at 296 K by Rothman et al. (2010).

The NO_2DSCD, O_4DSCD, and their respective errors are converted to the NO_2 profile and column using the retrieval algorithm, Mexican MAX-DOAS Fit (MMF; Friedrich et al. 2019). As reported by Friedrich et al. (2019), the aerosol extinction coefficient profile is retrieved using the known O_4 profile. Then, the NO_2 profile is retrieved. A priori information for aerosol and NO_2 profiles was set to decrease exponentially from the surface. A priori aerosol data for total optical depth, single scattering albedo, asymmetry parameter, and angstrom exponent were fixed respectively as 0.18, 0.95, 0.65, and 1.00. Wavelengths of 474 nm and 477 nm were used, respectively, for NO_2 and aerosol retrieval. Vertical resolution near the surface is more of the order of a couple of hundred meters. It reaches roughly a kilometer or even coarser around 1.5−2.5 km (Tirpitz et al. 2021). The total error of the NO_2VCD retrieved by MMF was estimated as approximately 20% (Friedrich et al. 2019). The effective distance of MAX-DOAS for 29 November 2018 was approx. 12−20 km.

2.2 Direct 3-D wind observation by 3-D CDL

Direct 3-D wind and aerosol (SNR) observations were conducted using a 3-D CDL (Mitsubishi Electric Corp.) installed at Fukuoka University (33.55°N, 130.37°E; 55 m above sea level) (Fig. 1). The 3-D CDL performs plan position indicator (PPI) scans continuously at 0°, 2°, and 10° and range height indicator (RHI) scans at 0° (northward) and 112° (clockwise from north). Then PPI scans with elevation angles of 0°, 2°, and 10° (five scans: 0°, 0°, 2°, 10°, 0°), and RHI scans with azimuth angles of 0° (north) and 112° (clockwise from north) (eight scans: 0°, 0°, 0°, 0°, 112°, 112°, 112°, 112°) were conducted in sequence. The scanning speed was 2° s^{-1}; a PPI (RHI) scan takes about 3 (1.5) min. For this study, we used PPI scans of the horizontal section (elevation angle = 0°) and RHI scans of the vertical north–south section (azimuth angle = 0°). The 3-D CDL has 200 range bins. The range resolution was set to 60 m. Thereby, the measurable distance was up to 12 km. Because of the shadows of buildings and mountains, we are unable to receive meaningful signals to the northwest/west/southwest/south in the PPI scans and RHI scans (Fig. 3). Because SNR decreases sharply along with increased distance from the lidar, we used radial wind velocity data with a threshold of SNR ≥ 8 dB to analyze the radial velocity variations in the boundary layer within an approx. 5 km horizontal area covering the Fukuoka urban area. Details of the setup and technical performance of 3-D CDL are described by Takashima et al. (2019).

3. Results and discussion

Figure 2 shows the NO_2 volume mixing ratio observed using MAX-DOAS at (a) Yakuin and (b) Fukuoka University on 29 November 2018 as a function of time (x-axis) and height above the ground (y-axis). At Yakuin, maximum NO_2 was observed near the surface at around 7:00−10:00. A minimum of NO_2 concentration was observed above the surface during 13:30−15:00. At Fukuoka University, a maximum was observed near the surface at 7:00−12:30. Higher contents of NO_2 appeared gradually at higher altitudes during 10:30−12:00. A minimum was observed above the surface at 14:00−16:30 (about 30 min later than at Yakuin). From these NO_2 variations, the 3-D wind field can be described by 3-D CDL in three phases: (i) 7:00−10:30, (ii) 10:30−13:30, and (iii) 13:30−17:00.

Figure 3 presents horizontal sections of radial wind velocity (m s^{-1}) with elevation angle of 0° and north–south height sections of radial wind velocity (m s^{-1}) with the azimuth direction of 0°, with representative snapshots corresponding to phases (i), (ii), and (iii). Near the surface, PPI scans revealed the following: (i) southeasterly winds of about 1−2 m s^{-1} (Fig. 3a), (ii) weak winds with a fishnet-like structure (Fujiwara et al. 2010) (Fig. 3b), and (iii) northerly winds of about 3−5 m s^{-1} (Fig. 3c). In the north–south

section, RHI scans revealed the following: (i) southerly winds in the thin layer up to about 0.2 km (Fig. 3d); (ii) disappearance of southerly winds in the thin layer and weak winds, at least until about 1.0 km (Fig. 3e); and (iii) northerly winds of about 3−5 m s^{-1} up to about 0.6 km (Fig. 3f).

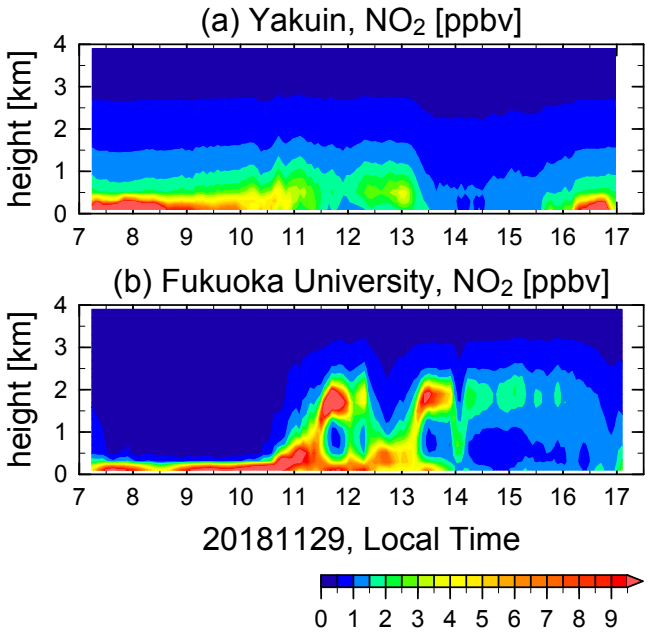

Fig. 2. Time–height section of NO_2 volume mixing ratio (ppbv) observed using MAX-DOAS at (a) Yakuin and (b) Fukuoka University on 29 November 2018.

The spatiotemporal variation of NO_2 is explainable by the results of 3-D wind fields: in phase (i), the airmass with high NO_2 concentrations emitted in the morning (around 7:00−10:30) was trapped in the thin layer near the surface. It was unable to mix vertically with the overlying clean airmass. In addition, high NO_2 concentrations in the airmass observed under southerly wind conditions are expected to originate mainly from Fukuoka city itself. In phase (ii), the thin layer near the surface has disappeared. The airmass with high NO_2 concentrations at the city center was transported upward from near the surface under weak horizontal wind conditions. It is noteworthy that the vertical transport/dilution speed estimated from Fig. 2b was approx. 0.5 m s^{-1} (10:30−11:40), which is comparable to the spatial average of the vertical velocity observed using 3-D CDL in Fig. 3e (< 1 m s^{-1}). In phase (iii), an airmass with high NO_2 concentration over the city center and an airmass with low NO_2 concentration over Hakata Bay advected southward (landward) by sea breezes in the afternoon. Yakuin is located seaside: a minimum NO_2 was observed about 30 min earlier than at Fukuoka University. The time difference between the two observatories is consistent with the northerly wind of about 3−5 m s^{-1} during phase (iii). The case of 29 November 2018 suggests that a combination of multiple MAX-DOAS and 3-D CDL is a powerful tool for understanding horizontal–vertical transport processes of NO_2 in urban areas.

Radiosonde observations are conducted routinely by the Fukuoka District Meteorological Observatory at Roppon-matsu (33.58°N, 130.38°E). At about 8:30 am, strong temperature inversion was observed below about 0.2 km (Fig. S2). The results are consistent with the high NO_2 concentrations near the surface during phase (i) because of the lack of mixing with airmasses located at higher altitudes.

Tropospheric NO_2VCD was observed by TROPOMI (KNMI, OFFLINE Level-2. Van Geffen et al. 2019) over Fukuoka city at 13:44 (local time) 29 November 2018 (Fig. S3). Comparisons

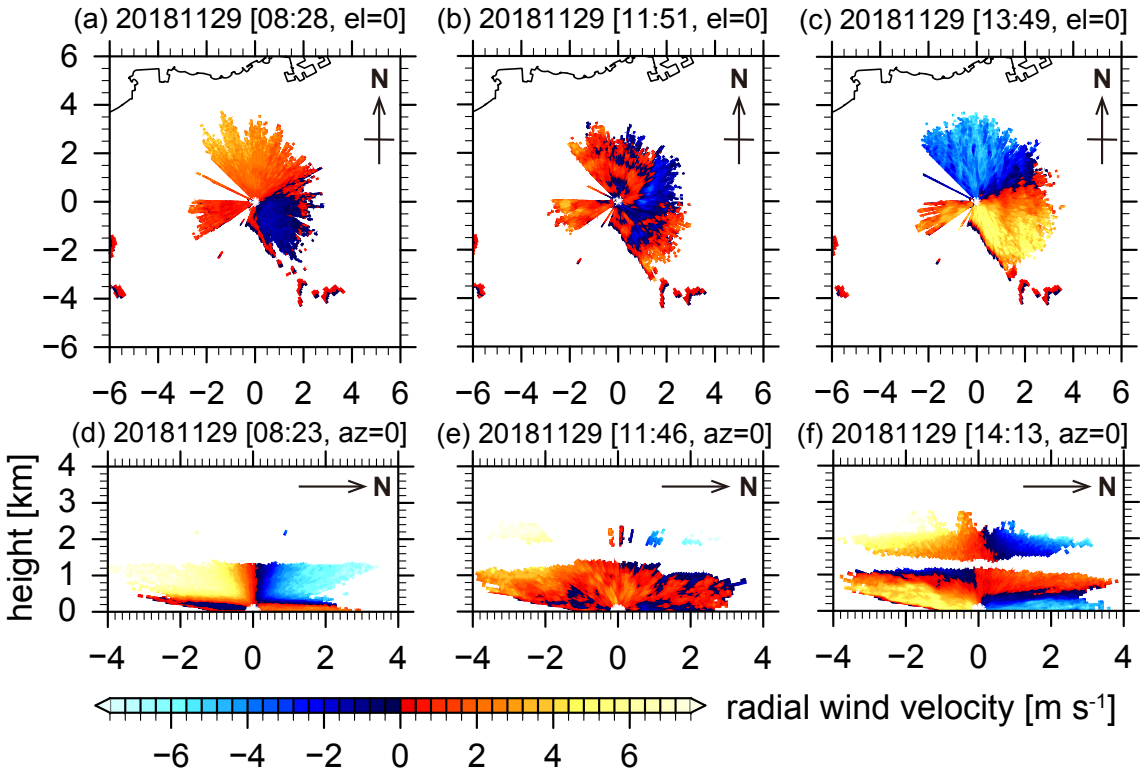

Fig. 3. Horizontal sections of radial wind velocity (m s^{-1}) for PPI scan with elevation angle of 0° at 8:28, 11:51, and 13:49 (top panels) and north–south height sections of radial wind velocity (m s^{-1}) for RHI with azimuth direction of 0° at 8:23, 11:46, and 14:13 (bottom panels) observed on 29 November 2018 by 3-D CDL in Fukuoka. For the top panels, axes show horizontal distance (km) from 3-D CDL. For bottom panels, the horizontal axis is distance (km) from 3-D CDL. The vertical axis shows height (km). Warm colors represent flow away from 3-D CDL. Cold colors represent flow toward it.

of tropospheric NO_2VCD by TROPOMI with both MAX-DOAS showed that the horizontal variations of NO_2VCD by TROPOMI were comparable with the horizontal variations of NO_2VCD by multiple MAX-DOAS. However, TROPOMI underestimates the tropospheric NO_2VCD as much as the Ozone Monitoring Instrument (OMI) described in Kanaya et al. (2014).

The NO_2 profile retrieved from MAX-DOAS measurements includes large retrieval error caused by smoothing and measurement noise. It also depends on the a priori profile and the assumed covariance matrix. As demonstrated by results of this study, large differences in NO_2 profiles (e.g., between the phases (i) (ii), and (iii)) were consistent with the vertical wind structure observed by 3-D CDL. These results and continuous MAX-DOAS measurements at multiple locations together with 3-D CDL are expected to contribute to improvement of NO_2 retrieval algorithms over urban areas for satellite observations.

4. Conclusions

To clarify three-dimensional spatiotemporal variations and horizontal–vertical transport processes of NO_2 over the urban area, the combination of NO_2 profile observations by multiple MAX-DOAS and direct wind observations by 3-D CDL was conducted over metropolitan Fukuoka in Japan.

Enhanced NO_2 contents were often observed over the city center. We conducted a case study on 29 November 2018 under clear sky conditions, when the NO_2 profiles were well retrieved. By providing direct observational evidence of a 3-D wind field, we clarified that, at the beginning, the airmass with high NO_2 concentrations was trapped within the thin layer near the surface. Then the airmass with high NO_2 concentrations was transported upward/diluted in the boundary layer by Bénard-type convection (fish net structure). Finally, the airmass with high NO_2 concentration over the city center and the airmass with low NO_2 concentration over the sea were advected by sea breezes in the boundary layer. The combination of multiple MAX-DOAS and 3-D CDL is a powerful tool for elucidating horizontal–vertical transport processes in urban areas.

We also compared the tropospheric NO_2VCD observed by TROPOMI to results of measurements obtained using the two MAX-DOAS instruments. Horizontal variations of NO_2VCD by TROPOMI were comparable with the horizontal variations of NO_2VCD by multiple MAX-DOAS. However, TROPOMI underestimates the tropospheric NO_2VCD.

This study validated the spatiotemporal variation of NO_2 for one day only, but long-term validation using multiple MAX-DOAS and 3-D CDL is expected to contribute to improving satellite retrieval in urban areas.

Acknowledgments

We thank Caroline Fayt, Michel Van Roozendael, and Thomas Danckaert for free use of the QDOAS software. We also thank Robert Spurr for free use of the VLIDORT radiative transfer code package. We extend our appreciation to Yasushi Fujiyoshi, Yugo Kanaya, and two anonymous reviewers for their useful and constructive comments. This work was supported in part by the JSPS KAKENHI (grant No. 17K00529), the fund from Fukuoka University (No. 197103). We used Sentinel-5 Precursor/TROPOMI satellite tropospheric NO_2 products retrieved by the Royal Netherlands Meteorological Institute (KNMI). The figures were produced using the GFD-Dennou Library.

Edited by: H. Irie

Supplements

Supplement 1: Photographs of MAX DOAS instrument used for this study. The telescope can be rotated to point at different elevation angles (2°, 3°, 4°, 5°, 10°, 20°, 30°, and 90°) to measure scattered sunlight.

Supplement 2: Vertical profiles of temperature (K), potential temperature (Po. Temp) (K) and relative humidity (%) observed by radiosonde in Roppon-matsu (33.58°N, 130.38°E) around 8:30 am, 29 November 2018.

Supplement 3: Longitude–latitude section of tropospheric NO_2VCD (10^{15} molecule cm^{-2}) observed by Sentinel-5 Precursor/TROPOMI on 29 November 2018. Colored square symbols represent tropospheric NO_2VCD.

References

Boersma, K. F., H. J. Eskes, and E. J. Brinksma, 2004: Error analysis for tropospheric NO_2 retrieval from space. *J. Geophys. Res.*, **109**, D04311, doi:10.1029/2003JD003962.

Boersma, K. F., H. J. Eskes, R. J. Dirksen, R. J. van der A, J. P. Veefkind, P. Stammes, V. Huijnen, Q. L. Kleipool, M. Sneep, J. Class, J. Leitão, A. Richter, Y. Zhou, and D. Brunner, 2011: An improved tropospheric NO_2 column retrieval algorithm for the Ozone Monitoring Instrument. *Atmos. Meas. Tech.*, **4**, 1905−1928, doi:10.5194/amt-4-1905-2011.

Bogumil, K., J. Orphal, T. Homann, S. Voigt, P. Spietz, O. C. Fleischmann, A. Vogel, M. Hartmann, H. Kromminga, H. Bovensmann, J. Frerick, and J. P. Burrows, 2003: Measurements of molecular absorption spectra with the SCIAMACHY pre-flight model: Instrument characterization and reference data for atmospheric remote-sensing in the 230−2380 nm region. *J. Photochem. Photobiol. A: Chem.*, **157**, 167−184, doi:10.1016/S1010-6030(03)00062-5.

Brinksma, E. J., G. Pinardi, H. Volten, R. Braak, A. Richter, A. Schönhardt, M. van Roozendael, C. Fayt, C. Hermans, R. J. Dirksen, T. Vlemmix, A. J. C. Berkhout, D. P. J. Swart, H. Oetjen, F. Wittrock, T Wagner, O. W. Ibrahim, G. de Leeuw, M. Moerman, R. L. Curier, E. A. Celarier, A. Cede, W. H. Knap, J. P. Veefkind, H. J. Eskes, M. Allaart, R. Rothe, A. J. M. Piters, and P. F. Levelt, 2008: The 2005 and 2006 DANDELIONS NO_2 and aerosol intercomparison campaigns. *J. Geophys. Res.*, **113**, D16S46, doi:10.1029/2007JD008808.

Friedrich, M. M., C. Rivera, W. Stremme, Z. Ojeda, J. Arellano, A. Bezanilla, J. A. García-Reynoso, and M. Grutter, 2019: NO_2 vertical profiles and column densities from MAX-DOAS measurements in Mexico City. *Atmos. Meas. Tech.*, **12**, 2545−2565, doi:10.5194/amt-12-2545-2019.

Frieß, U., P. S. Monks, J. J. Remedios, A. Rozanov, R. Sinreich, T. Wagner, and U. Platt, 2006: MAX-DOAS O_4 measurements: A new technique to derive information on atmospheric aerosols: 2. Modeling studies. *J. Geophys. Res. Atmos.*, **111**, D14203, doi:10.1029/2005JD006618.

Fujiwara, C., K. Yamashita, M. Nakanishi, and Y. Fujiyoshi, 2011: Dust devil-like vortices in an urban area detected by a 3D scanning Doppler lidar. *J. Appl. Meteor. Climatol.*, **50**, 534−547, doi:10.1175/2010JAMC2481.1.

van Geffen, J. H. G. M., H. J. Eskes, K. F. Boersma, J. D. Maasakkers, and J. P. Veefkind, 2019: TROPOMI ATBD of the total and tropospheric NO_2 data products (issue 1.4.0), Royal Netherlands Meteorological Institute (KNMI), De Bilt, the Netherlands, s5P-KNMI-L2-0005-RP. (Available online at: http://www.tropomi.eu/sites/default/files/files/publicSentinel-5P-TROPOMI-ATBD-NO_2-data-products.pdf, accessed 17 August 2020)

Hilboll, A., A. Richter, and J. P. Burrows, 2013: Long-term changes of tropospheric NO_2 over megacities derived from multiple satellite instruments. *Atmos. Chem. Phys.*, **13**, 4145−4169, doi:10.5194/acp-13-4145-2013.

Hönninger, G., C. von Friedeburg, and U. Platt, 2004: Multi Axis Differential Optical Absorption Spectroscopy (MAX-DOAS). *Atmos. Chem. Phys.*, **4**, 231−254, doi:10.5194/acp-4-231-2004.

Irie, H., Y. Kanaya, H. Akimoto, H. Tanimoto, Z. Wang, J. F.

Gleason, and E. J. Bucsela, 2008: Validation of OMI tropospheric NO_2 column data using MAX-DOAS measurements deep inside the North China Plain in June 2006: Mount Tai Experiment 2006. *Atmos. Chem. Phys.*, **8**, 6577−6586, doi:10.5194/acp-8-6577-2008.

Irie, H., H. Takashima, Y. Kanaya, K. F. Boersma, L. Gast, F. Wittrock, D. Brunner, Y. Zhou, and M. Van Roozendael, 2011: Eight-component retrievals from ground-based MAX-DOAS observations. *Atmos. Meas. Tech.*, **4**, 1027−1044, doi:10.5194/amt-4-1027-2011.

Kanaya, Y., H. Irie, H. Takashima, H. Iwabuchi, H. Akimoto, K. Sudo, M. Gu, J. Chong, Y. J. Kim, H. Lee, A. Li, F. Si, J. Xu, P. H. Xie, W. Q. Liu, A. Dzhola, O. Postylyakov, V. Ivanov, E. Grechko, S. Terpugova, and M. Panchenko, 2014: Long-term MAX-DOAS network observations of NO_2 in Russia and Asia (MADRAS) during the period 2007−2012: Instrumentation, elucidation of climatology, and comparisons with OMI satellite observations and global model simulations. *Atmos. Chem. Phys.*, **14**, 7909−7927, doi:10.5194/acp-14-7909-2014.

Lamsal, L. N., R. V. Martin, A. van Donkelaar, E. A. Celarier, E. J. Bucsela, K. F. Boersma, R. Dirksen, C. Luo, and Y. Wang, 2010: Indirect validation of tropospheric nitrogen dioxide retrieved from the OMI satellite instrument: Insight into the seasonal variation of nitrogen oxides at northern midlatitudes. *J. Geophys. Res.*, **115**, D05302, doi:10.1029/2009JD013351.

Ma, J. Z., S. Beirle, J. L. Jin, R. Shaiganfar, P. Yan, and T. Wagner, 2013: Tropospheric NO_2 vertical column densities over Beijing: results of the first three years of ground-based MAX-DOAS measurements (2008−2011) and satellite validation. *Atmos. Chem. Phys.*, **13**, 1547−1567, doi:10.5194/acp-13-1547-2013.

Miyazaki, K., H. J. Eskes, and K. Sudo, 2012: Global NOx emission estimates derived from an assimilation of OMI tropospheric NO_2 columns. *Atmos. Chem. Phys.*, **12**, 2263−2288, doi:10.5194/acp-12-2263-2012.

Pinardi, G., M. Van Roozendael, F. Hendrick, N. Theys, N. Abuhassan, A. Bais, F. Boersma, A. Cede, J. Chong, S. Donner, T. Drosoglou, A. Dzhola, H. Eskes, U. Frieß, J. Granville, J. Herman, R. Holla, J. Hovila, H. Irie, Y. Kanaya, D. Karagkiozidis, N. Kouremeti, J.-C. Lambert, J. Ma, E. Peters, A. Piters, O. Postylyakov, A. Richter, J. Remmers, H. Takashima, M. Tiefengraber, P. Valks, T. Vlemmix, T. Wagner, and F. Wittrock, 2020: Validation of tropospheric NO_2 column measurements of GOME-2A and OMI using MAX-DOAS and direct sun network observations. *Atmos. Meas. Tech.*, **13**, 6141−6174, doi:10.5194/amt-13-6141-2020.

Platt, U., 1994: *Differential Optical Absorption Spectroscopy (DOAS)*. John Wiley & Sons, **127**, 27−83 pp.

Richter, A., J. P. Burrows, H. Nüß, C. Granier, and U. Niemeier, 2005: Increase in tropospheric nitrogen dioxide over China observed from space. *Nature*, **437**, 129−132, doi:10.1038/nature04092.

Rothman, L. S., I. E. Gordon, R. J. Barber, H. Dothe, R. R. Gamache, A. Goldman, V. I. Perevalov, S. A. Tashkun, and J. Tennyson, 2010: HITEMP, the high-temperature molecular spectroscopic database. *J. Quant. Spectrosc. Radiat. Transf.*, **111**, 2139−2150, doi:10.1016/j.jqsrt.2010.05.001.

Seinfeld, J. H., and S. N. Pandis, 1998: *Atmospheric Chemistry and Physics, from Air Pollution to Climate Change*. John Wiley, New York, 131−134 pp.

Sinreich, R., U. Frieß, T. Wagner, and U. Platt, 2005: Multi axis differential optical absorption spectroscopy (MAX-DOAS) of gas and aerosol distributions. *Faraday Discuss.*, **130**, 153−164, doi:10.1039/b419274p.

Solomon, S., R. W. Portmann, R. W. Sanders, J. S. Daniel, W. Madsen, B. Bartram, and E. G. Dutton, 1999: On the role of nitrogen dioxide in the absorption of solar radiation. *J. Geophys. Res. Atmos.*, **104**, 12047−12058, doi:10.1029/1999 JD 900035.

Takashima, H., K. Hara, C. Nishita-Hara, Y. Fujiyoshi, K. Shiraishi, M. Hayashi, A. Yoshino, A. Takami, and A. Yamazaki, 2019: Short-term variation in atmospheric constituents associated with local front passage observed by a 3-D coherent Doppler lidar and in-situ aerosol/gas measurements. *Atmos. Environ. X.*, **3**, 100043, doi:10.1016/j.aeaoa.2019.100043.

Takashima, H., Y. Kanaya, and H. Irie, 2015: Spatiotemporal inhomogeneity in NO_2 over Fukuoka observed by ground-based MAX-DOAS. *Atmos. Environ.*, **100**, 117−123, doi:10.1016/j.atmosenv.2014.10.057.

Thalman, R., and R. Volkamer, 2013: Temperature dependent absorption cross-sections of O_2−O_2 collision pairs between 340 and 630 nm and at atmospherically relevant pressure. *Phys. Chem. Chem. Phys.*, **15**, 15371−15381, doi:10.1039/c3cp50968k.

Tirpitz, J. L., U. Frieß, F. Hendrick, C. Alberti, M. Allaart, A. Apituley, A. Bais, S. Beirle, S. Berkhout, K. Bognar, T. Bösch, I. Bruchkouski, A. Cede, K. L. Chan, M. den Hoed, S. Donner, T. Drosoglou, C. Fayt, M. M. Friedrich, A. Frumau, L. Gast, C. Gielen, L. Gomez-Martín, N. Hao, A. Hensen, B. Henzing, C. Hermans, J. Jin, K. Kreher, J. Kuhn, J. Lampel, A. Li, C. Liu, H. Liu, J. Ma, A. Merlaud, E. Peters, G. Pinardi, A. Piters, U. Platt, O. Puentedura, A. Richter, S. Schmitt, E. Spinei, D. Stein Zweers, K. Strong, D. Swart, F. Tack, M. Tiefengraber, R. van der Hoff, M. van Roozendael, T. Vlemmix, J. Vonk, T. Wagner, Y. Wang, Z. Wang, M. Wenig, M. Wiegner, F. Wittrock, P. Xie, C. Xing, J. Xu, M. Yela, C. Zhang, and X. Zhao, 2021: Intercomparison of MAX-DOAS vertical profile retrieval algorithms: Studies on field data from the CINDI-2 campaign. *Atmos. Meas. Tech.*, **14**, 1−35, doi:10.5194/amt-14-1-2021.

Valks, P., G. Pinardi, A. Richter, J.-C. Lambert, N. Hao, D. Loyola, M. Van Roozendael, and S. Emmadi, 2011: Operational total and tropospheric NO_2 column retrieval for GOME-2. *Atmos. Meas. Tech.*, **4**, 1491−1514, doi:10.5194/amt-4-1491-2011.

Vandaele, A. C., C. Hermans, P. C. Simon, M. Van Roozendael, J. M. Guilmot, M. Carleer, and R. Colin, 1996: Fourier transform measurement of NO_2 absorption cross-section in the visible range at room temperature. *J. Atmos. Chem.*, **25**, 289−305, doi:10.1007/BF00053797.

Veefkind, J. P., I. Aben, K. McMullan, H. Förster, J. de Vries, G. Otter, J. Claas, H. J. Eskes, J. F. de Haan, Q. Kleipool, M. van Weele, O. Hasekamp, R. Hoogeveen, J. Landgraf, R. Snel, P. Tol, P. Ingmann, R. Voors, B. Kruizinga, R. Vink, H. Visser, and P. F. Levelt, 2012: TROPOMI on the ESA Sentinel-5 Precursor: A GMES mission for global observations of the atmospheric composition for climate, air quality and ozone layer applications. *Remote Sens. Environ.*, **120**, 70−83, doi:10.1016/j.rse.2011.09.027.

Wagner, T., B. Dix, C. V. Friedeburg, U. Frieß, S. Sanghavi, R. Sinreich, and U. Platt, 2004: MAX-DOAS O_4 measurements: A new technique to derive information on atmospheric aerosols – Principles and information content. *J. Geophys. Res.*, **109**, D22205, doi:10.1029/2004JD004904.

Wittrock, F., H. Oetjen, A. Richter, S. Fietkau, T. Medeke, A. Rozanov, and J. P. Burrows, 2004: MAX-DOAS measurements of atmospheric trace gases in Ny-Ålesund – Radiative transfer studies and their application. *Atmos. Chem. Phys.*, **4**, 955−966, doi:10.5194/acp-4-955-2004.

Yamaguchi, H., H. Takashima, and Y. Maruyama, 2016: Spatiotemporal Inhomogeneity in Nitrogen Dioxide (NO_2) over Fukuoka Observed by Car MAX-DOAS. *J. Jpn. Soc. Atmos. Environ.*, **51**, 238−244.

Manuscript received 30 November 2020, accepted 8 February 2021
SOLA: *https://www.jstage.jst.go.jp/browse/sola/*